

## USE OF GPS MULTICORRELATOR RECEIVERS FOR MULTIPATH PARAMETERS ESTIMATION

### ABSTRACT

The performance of GPS may be degraded by many perturbations such as jamming, the effects of the ionosphere, and multipath. Many studies have been done to reduce the effect of multipath on the GPS measurements. Some of these are based on the radiation pattern of the receiving antenna, while most of them concentrate on the characteristics of the receiver tracking loops. The advent of multicorrelator receivers widens the range of methods that can be considered to tackle this problem as in [1]. In particular, this enables the characterization of multipath effects on the tracking loops through the analysis of the shape of the correlation peak.

The aim of the proposed paper is to describe a least squares method to identify different multipath parameters using multicorrelator outputs, and to present results of the application of this technique.

The paper starts with a brief review of the impact of several reflected rays on the code and phase tracking loops. Then, the principle of multicorrelator receivers is described, and the particular structure of the multicorrelator firmware of the NovAtel Millennium receiver is given as an illustration. After this, the least squares technique used to estimate the relative amplitude, relative code and phase delays, code and phase tracking errors is presented. Results of the application of this technique on real data collected on a real receiver connected to a Spirent GPS generator are shown.

These results illustrate the overall good performance of the method and its limitations. Finally, a conclusion is drawn on this technique and its possible capacity to improve the performance of tracking loops by removing multipath components in correlator outputs.

### 1. MODEL AND IMPACT OF MULTIPATH

#### 1.1 Multipath model

The multipath phenomena are encountered in most radio propagation. This phenomenon happens when the received signal is a contribution of a direct ray and one or more other reflected rays, which follow indirect paths.

The effect depends on the application we deal with. In the case of the Global Positioning System (GPS), multipath deteriorate the tracking quality of both PLL and DLL inside the GPS receiver. Consequently, the system performance, especially its range measurement accuracy may be diminished dramatically, This measurement error caused by multipath ranges from centimeters to several meters,

In the case of GPS applications it is difficult to give a statistical model to describe the received signal in presence of multipath. However, many hypotheses can be made. For instance, the reflected signals are delayed with respect to the direct one, as they travel a longer path. Furthermore, only signals with a delay less than one chip are considered. This latter hypothesis may be justified by the fact that signals with a code delay larger than roughly one chip are uncorrelated with the direct ray. In addition, the reflected ray is supposed to have less power than the direct one.

In the presence of  $N-1$  reflected rays, the received signal at the input of the tracking loops may be written as follows:

$$s(t) = A \cdot \sum_{i=0}^{N-1} \alpha_i \cdot d(t - \tau_i) c_f(t - \tau_i) \cdot \cos(2\pi f_c t - \theta_i) \quad (1.1)$$

where

- $\alpha_i, \tau_i$  and  $\theta_i$  represent the amplitude, the time delay and the phase delay of the  $i^{\text{th}}$  path with respect to the direct one (the index zero is used for the direct path).
- $f_c$  is the carrier frequency

- $c_f(t)$  is the Pseudo Noise code waveform filtered by the RF front-end filter
- $d(t)$  represent the payload data.

## 1.2 Multipath effect

In the absence of multipath, the matched filter output is close to the symmetric correlation function of the PN code. This symmetry is needed to obtain reliable time delay estimation. Nevertheless, in the presence of multipath, this symmetry is lost (as shown in figure 1.1), consequently, the propagation delay becomes harder to estimate, thus, the range measurement accuracy is diminished.

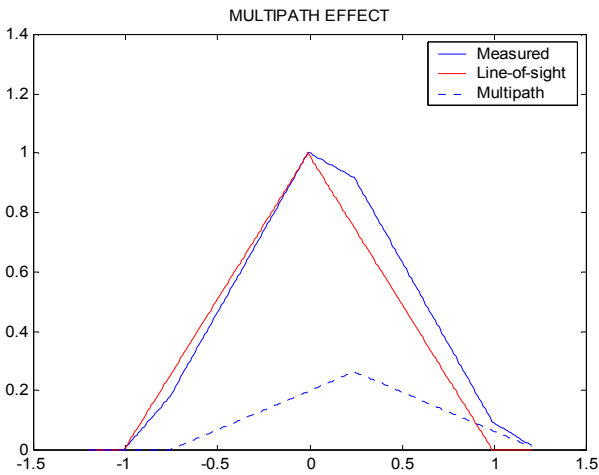


Figure 1.1 Multipath effect on the normalized correlation function.

For the sake of simplicity, the effect of multipath on the tracking loops is studied in the case of one and two reflected rays. The tracking error of both DLL and PLL is assessed as a function of the reflected rays parameters.

In the case of one reflected ray, the phase tracking error is given by equation 1.2 [2].

$$\tan(\theta_0 - \hat{\theta}_0) = \frac{\alpha_1 K_c(\tau_0 + \Delta\tau_1 - \hat{\tau}_0) \cdot \sin(\Delta\theta_1)}{K_c(\tau_0 - \hat{\tau}_0) + \alpha_1 \cos(\Delta\theta_1) K_c(\tau_0 + \Delta\tau_1 - \hat{\tau}_0)} \quad (1.2)$$

where

- $\Delta\theta = \theta - \theta_0$  is the phase difference between the reflected ray and the direct one.
- $\hat{\tau}_0$  is the propagation delay estimate
- $\hat{\theta}_0$  is the phase estimate of the direct signal.
- $K_c$  is the autocorrelation function of the filtered PN code.

From 1.2 we note that the tracking error depends on the code tracking error estimate, therefore, we better have a good time delay

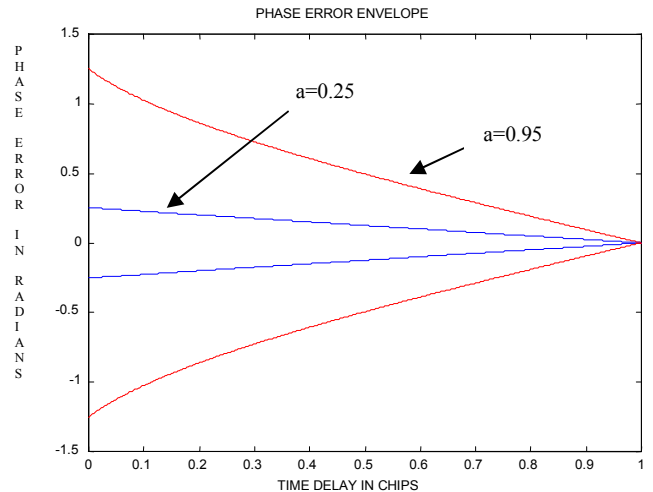
estimate. We note also that  $\Delta\theta=0$  yields null phase tracking error.

In general, only the phase tracking error envelope is given. The latter quantity gives a better grasp of the evolution of the phase tracking error. Furthermore, it is easier to represent. The error envelope is calculated for each multipath time delay by maximizing 1.2 as a function of  $\Delta\theta$ . To make this calculus feasible we have assumed perfect time synchronization *i.e.*  $\tau_0 = \hat{\tau}_0$  and an unlimited receiver filter bandwidth. Equation 1.3 gives the phase tracking error envelope as a function of the multipath time delay and its relative amplitude:

$$\tan(\theta_0 - \hat{\theta}_0) = \pm \frac{\alpha_1 \cdot (1 - \Delta\tau_1)}{\sqrt{1 - \alpha_1^2 (1 - \Delta\tau_1)^2}} \quad (1.3)$$

We note that that the equation above is well defined thanks to conditions made in subsection 1.1.

Figure 1.2 shows the phase tracking error envelope versus the multipath time delay for two multipath amplitudes.



In the situation of two reflected rays, the same envelope may be written as below:

$$\tan(\theta - \hat{\theta}) = \pm \frac{\alpha_1 \cdot (1 - \Delta\tau_1) + \alpha_2 \cdot (1 - \Delta\tau_2)}{\sqrt{1 - \alpha_1^2 \alpha_2^2 \cdot (1 - \Delta\tau_1)^2 (1 - \Delta\tau_2)^2}} \quad (1.4)$$

where  $\Delta\tau_i$  is the time delay of the  $i^{\text{th}}$ ,  $i \in \{1,2\}$ , reflected ray with respect to the direct one. Obviously, equation 1.4 may be generalized for more than two reflected rays.

In the case of the delay lock loop (DLL) it is not possible to give the exact formula of the delay tracking error introduced by multipath. However, analytical results of the error envelope may be given. To be closer to the practical situation, simulations are done in the case of limited bandwidth receiver filter. Figure 1.3 shows the delay tracking error envelope versus

the multipath time delay. Results are given for two chip spacings, multipath amplitude is unchanged. It can be shown that the time delay error is commensurate with the chip spacing, therefore, operating at low chip spacing values provides a good help to mitigate the degradation caused by multipath [3], [4]. We recall that this technique is also helpful to reduce the fluctuation of the code delay estimate caused by channel noise.

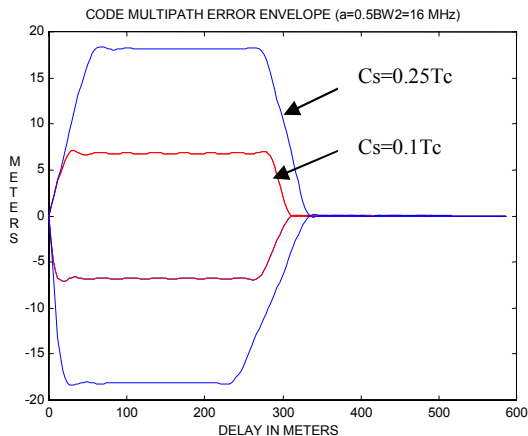


Figure 1.3 : code error envelope

## 2. MULTICORRELATOR RECEIVERS

Classical receivers offer several tracking channels, each of them being driven by two pairs of correlator outputs. A multicorrelator receiver provides values of the correlation of the incoming signal with several delayed replicas of the same local code in a single tracking channel. In that case, we get simultaneously several I and Q samples for each relative delay  $d$  of each replica with respect to punctual.

For the experiment described here, we have used a Novatel Millenium receiver whose software has been modified so as to provide 1 tracking channel delivering 48 correlators outputs on I and 48 outputs on Q.

The operations performed in each correlation channel are illustrated in figure 2.1.

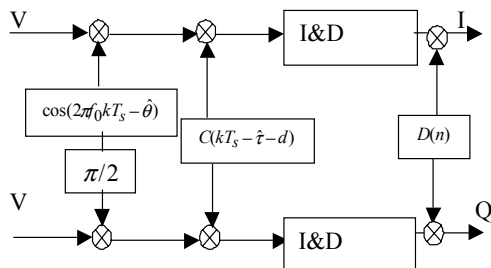


Figure 2.1: Architecture of one correlator output.

The distribution of the correlation points with respect to punctual can be chosen between 3 configurations: 'uniform', 'trailing edge' and 'peak intensive'. The shapes of these distributions are illustrated in figures 2.2, 2.3 and 2.4.

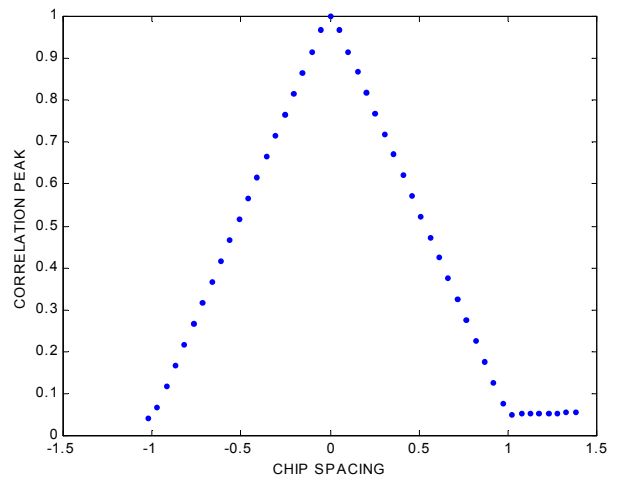


Figure 2.2 Samples sequence for 'uniform' distribution

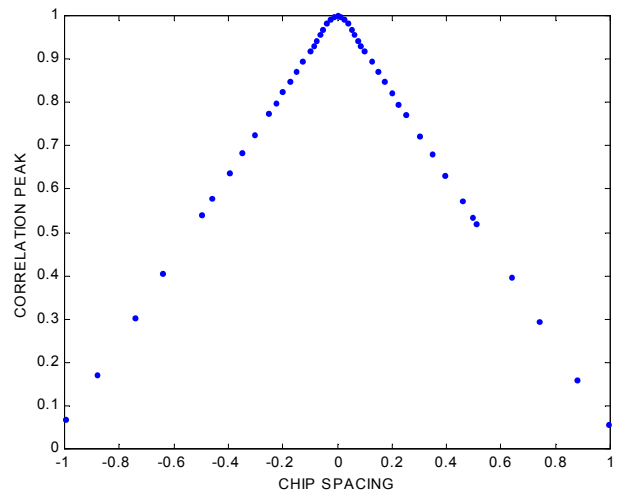


Figure 2.3 Samples sequence for 'peak intensive' distribution

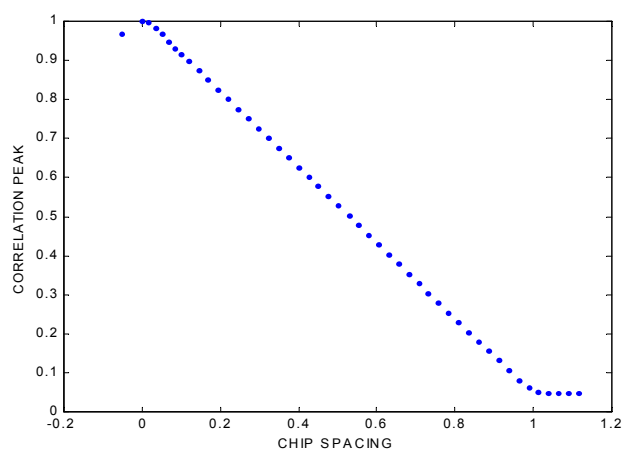


Figure 2.4 Samples sequence for 'trailing edge' distribution

These three configurations were used to evaluate the performance of our technique.

Example of the effect of multipath on the correlator outputs is shown in figure 2.5.

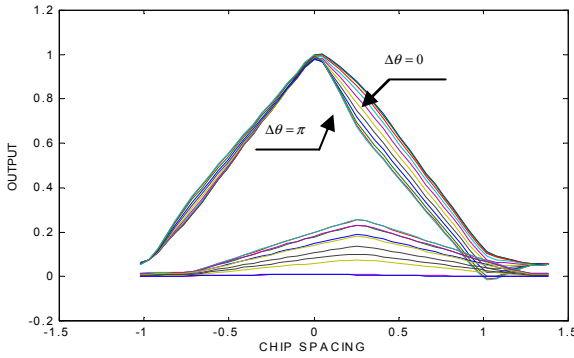


Figure 2.5 Example of I and Q correlator outputs variation as a function of reflected ray phase shift ( $\alpha = 0.25$ ,  $\Delta\tau_1 = 0.25$  chip).

### 3. USE OF THE LEAST SQUARE METHOD

#### 3.1 Principle

In the previous section, we have seen that the multicorrelator receiver we are using provides 48 samples of the correlation function for both in-phase and quadrature components of the Integrate & Dump filter outputs. Those 96 samples form the set of observations which is updated every second. The goal of the least squares method is to minimize the Euclidian distance between the observation and the mathematical model, then, we chose the MSE solution as an estimation of the multipath parameters and both phase and code tracking errors. We note that we deal with a non-linear model. Therefore, an iterative least squares method is used. In addition, in our algorithm, we have taken into account the channel noise contribution, thus, the iterative generalized least squares method has been adopted.

#### 3.2 The Least Squares Algorithm

Observation model may be mathematically expressed as follows:

$$Y_{obs}(k) = \sum_{i=1}^N \alpha_i K_c(d_k - \epsilon_\tau - \Delta\tau_i) \cos(\epsilon_\theta + \Delta\theta_i) + n(k) \quad (3.1)$$

$$k = 1, 2, \dots, 48$$

$$Y_{obs}(k) = \sum_{i=1}^N \alpha_i K_c(d_k - \epsilon_\tau - \Delta\tau_i) \sin(\epsilon_\theta + \Delta\theta_i) + n(k)$$

$$k = 49, 50, \dots, 96$$

- $n(k)$  refers to the noise terms

- $d = (d_i)_{i \leq 48}$  is the sampling instants vector normalized with respect to chip time duration.

Let  $X$  be the set of parameters we want to estimate. Then, observation  $Y$  may be related to  $X$  by a non-linear equation as follows:

$$Y_{obs} = h(X) + n \quad (3.2)$$

The inverse function of  $h$  can't be analytically calculated. Furthermore the noise term makes the calculation of the exact solution impossible. Consequently, we can only approximate the exact value. The estimator is the solution of the least square equation:

$$\hat{X} = \min_X \|Y_{obs} - h(X)\|^2 \quad (3.3)$$

As we are faced with a non-linear equation, an iterative method is the only possible way to estimate multipath parameters. The  $n+1$  order estimator is deduced from the  $n$ th order one by a linear function:

$$\hat{X}_{n+1} = \hat{X}_n + \delta X_n \quad (3.4)$$

Here,  $\delta X_n$  stands for the adjustment of the  $n$ th order estimator, it is given by:

$$\delta X_n = [H(\hat{X}_n)^T W H(\hat{X}_n)]^{-1} H(\hat{X}_n)^T W \delta Y \quad (3.5)$$

where

- $W$  is the inverse matrix of the noise covariance matrix
- $H(\hat{X}_n)$  is the gradient vector of  $h$  in vicinity of  $\hat{X}_n$ .
- $\delta Y = Y_{obs} - h(\hat{X}_n)$  is the measurement prediction error.

The iteration process is stopped when the Euclidian distance between observation and model is smaller than a fixed threshold.

#### 3.3 Theoretical performance

The theoretical performance of a least squares algorithm depends on the condition number of the gradient matrix of the observation model. Let  $H$  be a matrix, the condition number of  $H$  is defined by  $\mu = \frac{\mu_+}{\mu_-}$ , where  $\mu_+$  (respectively  $\mu_-$ ) denotes the largest (respectively the smallest) eigenvalue of the matrix  $H^T H$  and  $H^T$  is the hermitian transpose matrix of  $H$ . Large condition numbers indicate a nearly singular matrix.

The effect of the multipath parameters, namely the multipath time and phase delays on the condition number were assessed. The results

give us an idea about the singularity of the gradient matrix.

The smallest the condition number is, the easier the MSE equation to solve is.

Figures 3.1 and figure 3.2 show the condition number variation as a function of multipath amplitude, delay and phase.

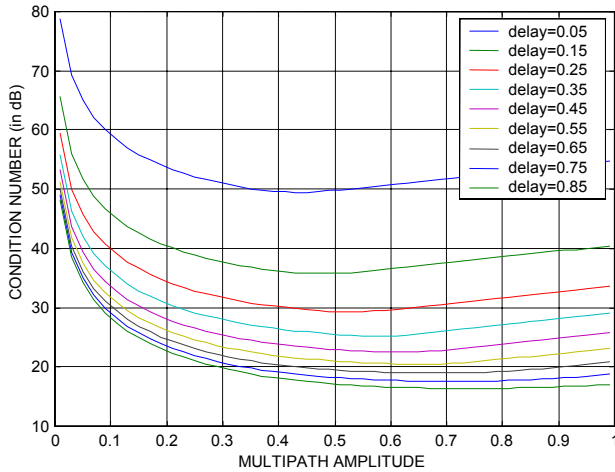


Figure 3.1 Condition number versus multipath time delay

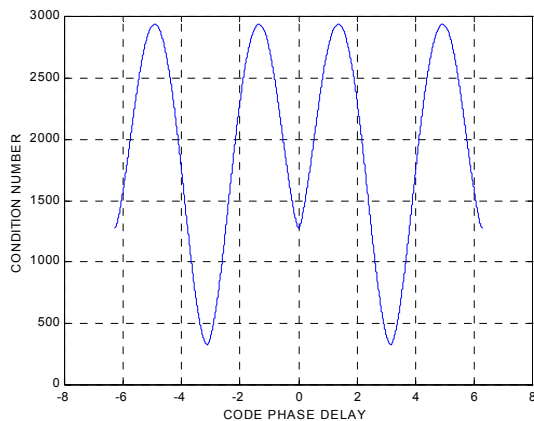


Figure 3.2 Condition number versus multipath phase delay

As we see from figure 3.1, the multipath parameters are harder to estimate for small multipath time delays. This conclusion is obvious because reflected rays with small delays are very close to the direct one. Moreover, we have found that small multipath parameters yield large condition number, consequently, the estimation of those multipath is more difficult.

In addition, as shown in figure 3.2, parameters are harder to estimate when the reflected ray is in quadrature with respect to the direct one.

In the case of two reflected rays, the condition number is calculated as a function of the difference time delay between those two rays. We have concluded that the algorithm

efficiency is diminished for small time differences. In fact, such a situation introduces an ambiguity when we try to separate the two signals simply because the observation function is not injective (i.e. two different sets of multipath parameters can yield to the same vector of I and Q correlation samples).

Figure 3.3 shows the evaluation of the condition number versus the first time delay, the second time delay is taken as constant and equal to 0.45.

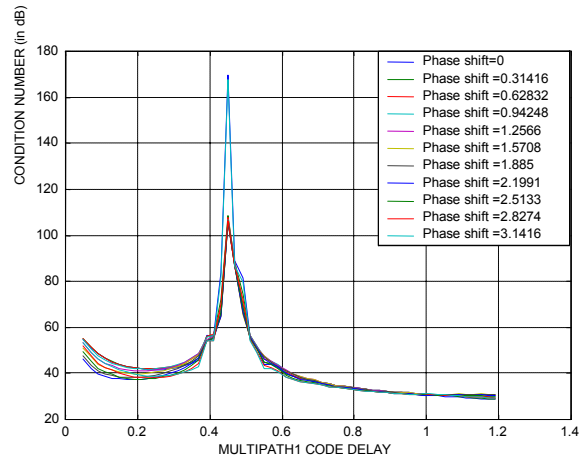


Figure 3.3 Condition number versus the first multipath time delay.

## 4. RESULTS WITH A REAL RECEIVER

### 4.1 Signal generation

The GPS signal we process is provided by a SPIRENT GPS signal generator **GSS 2760**. Then, it is fed to a Novatel Multicorrelator GPS receiver. Subsequently, the correlator outputs are stored into a computer. Our MSE algorithm will process obtained raw data in order to estimate multipath parameters. We note that those parameters are defined in the scenario inserted in the GSS 2760.

### 4.2 Scenario with one reflected ray

In the case of only one reflected ray, the multipath signal is characterised by a fixed amplitude throughout the scenario. The time delay with respect to the direct ray ranges from 0 to 1.2  $T_c$ . That time delay varies by slices of 30 s: it is constant during 30 seconds, then increased by 0.02  $T_c$ , then again kept constant during 30s, etc...

The phase shift of the reflected ray has a linear variation versus time. The slope is equal to  $2\pi$  in 10 s. The latter scenario was run for 3 amplitude values (0.25, 0.1 and 0.05) and for the three different receiver configurations. Major results are illustrated by the following figures.

Figures 4.1, 4.2, 4.3 and 4.4 show estimates of multipath code, amplitude, phase, code and phase tracking errors in the case of the 'uniform distribution' receiver configuration with a multipath amplitude set to 0.1.

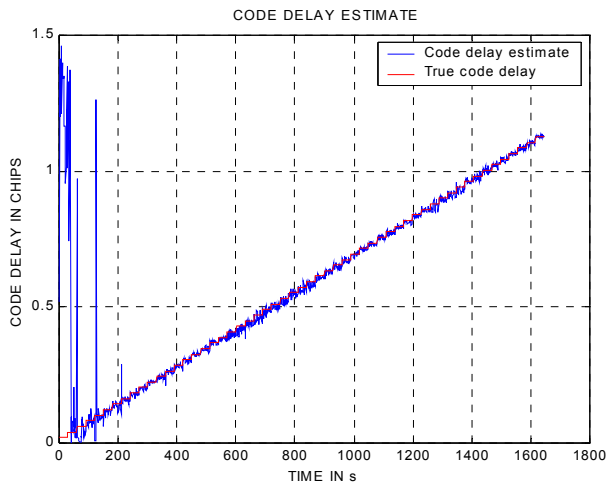


Figure 4.1 Multipath time delay estimation performance with 'uniform' receiver configuration for  $\alpha = 0.1$  as a function of time in the run (multipath delay varies by 0.02 chip every 30 s).

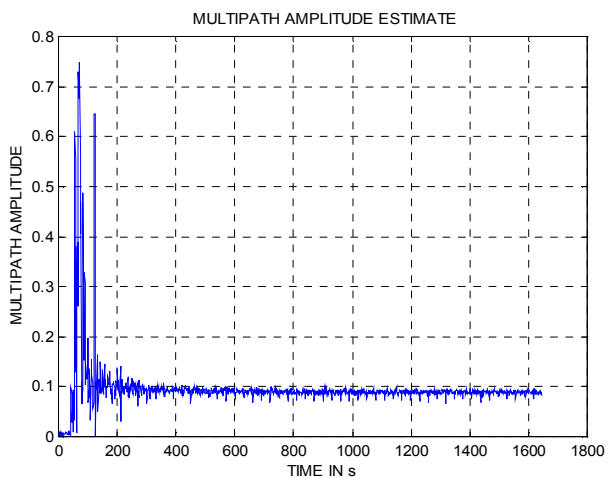


Figure 4.2 Multipath amplitude estimation performance with 'uniform' receiver configuration for  $\alpha = 0.1$  as a function of time in the run (multipath delay varies by 0.02 chip every 30 s).

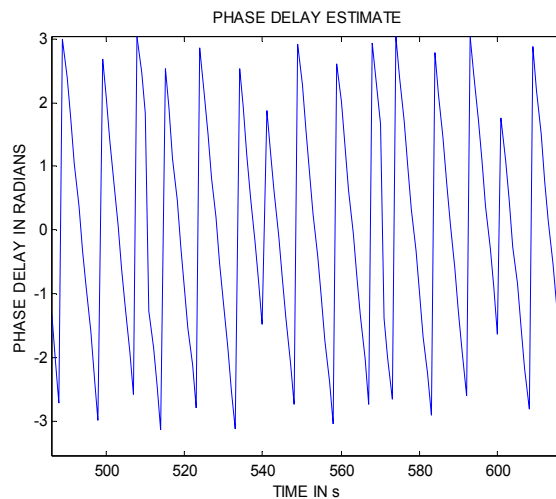


Figure 4.3 Zoom of multipath phase delay estimation performance with 'uniform' receiver configuration for  $\alpha = 0.1$  as a function of time in the run (multipath delay varies by 0.02 chip every 30 s).

Those figures show the quality of the multipath parameters estimation (code delay, amplitude, phase). As we can see in figure 4.1, the multipath time delay is estimated with an accuracy close to 0.05 chip (14 m) when that delay is larger than 0.1 chip. When the multipath time delay is lower than 0.1 chip, the estimation is not robust. Similarly, we can see in figure 4.2 that the amplitude estimate is very good (accuracy better than 0.05) when the multipath delay is larger than 0.1 chip. When the delay is smaller than 1 chip, the amplitude estimation is not robust. As shown in figure 4.3, the phase estimate is also very good, displaying a linear evolution with sudden phase shifts every 30 s.

Figure 4.4 shows the evolution of the code and phase tracking error estimates. We can see that, in line with theory, these two estimates are in quadrature [2]. In addition, the phase tracking error changes suddenly every 30 s. The code tracking error estimate is more affected by noise than the phase tracking error estimate.

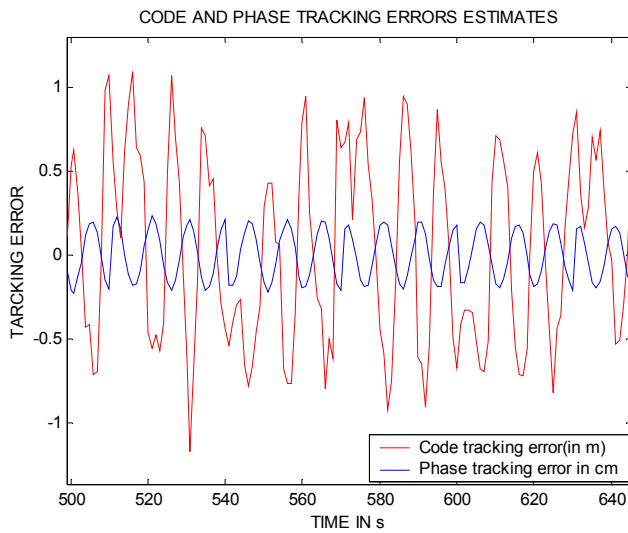


Figure 4.4 Code and phase tracking error estimates with 'uniform' receiver configuration for  $\alpha = 0.1$  as a function of time in the run (multipath delay varies by 0.02 chip every 30 s).

Figures 4.5 and 4.6 show the code and phase tracking error estimates as a function of the multipath delay. These estimates are compared with the exact theoretical tracking error envelope. As we can see, the code tracking error estimate is very close to the theoretical envelope when the delay is lower than 0.1 chip (30 m). As already seen in figure 4.4, the phase tracking error estimate is very close to theory whatever the multipath time delay.

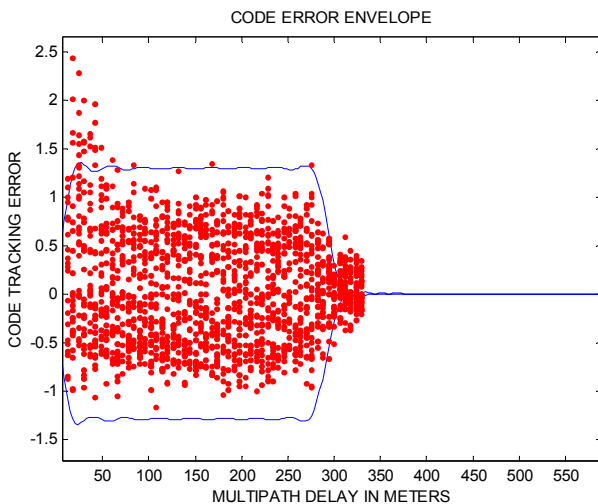


Figure 4.5 Time tracking error estimate envelope with 'uniform' receiver configuration for  $\alpha = 0.1$  as a function multipath delay.

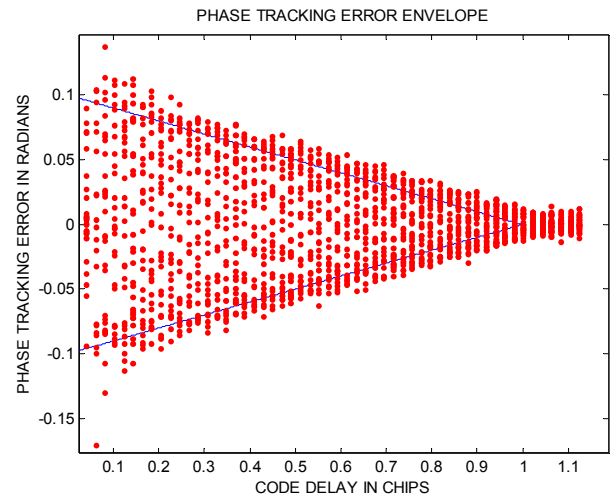


Figure 4.6 Time tracking error estimate envelope with 'uniform' receiver configuration for  $\alpha = 0.1$  as a function multipath delay.

The performance of the estimation is degraded when the relative multipath amplitude is low. Figure 4.7 (to be compared with figure 4.1) shows the time delay estimate when the multipath relative amplitude is equal to 0.05. As we can see, that estimate is noisier than when  $\alpha = 0.1$ .

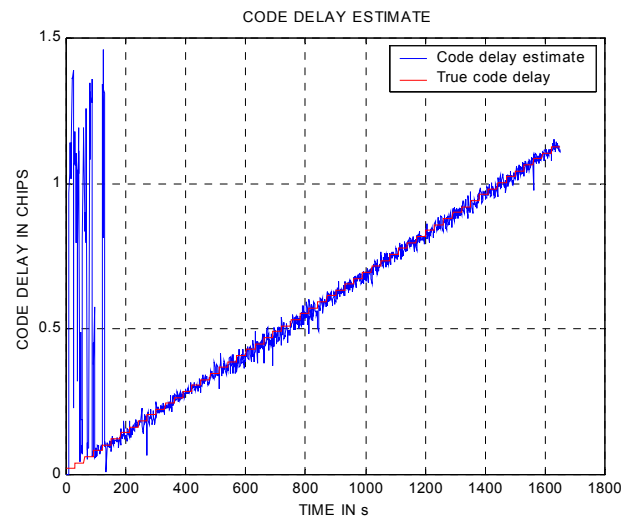


Figure 4.7 Multipath time delay estimation performance with 'uniform' receiver configuration for  $\alpha = 0.05$  as a function of time in the run (multipath delay varies by 0.02 chip every 30 s).

The results obtained with other receiver configurations have slightly the same behaviour. Figures 4.8 and 4.9 show the time delay and amplitude estimate with the 'trailing edge' receiver configuration.

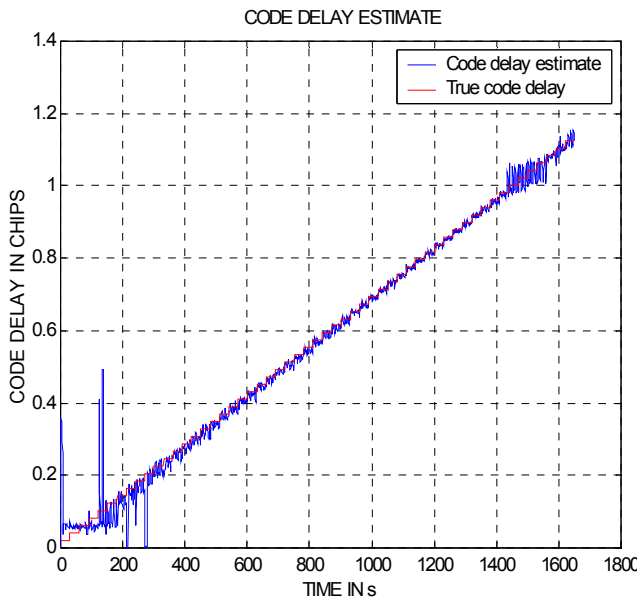


Figure 4.8 Multipath time delay estimation performance with ‘trailing edge’ receiver configuration for  $\alpha = 0.1$  as a function of time in the run (multipath delay varies by 0.02 chip every 30 s).

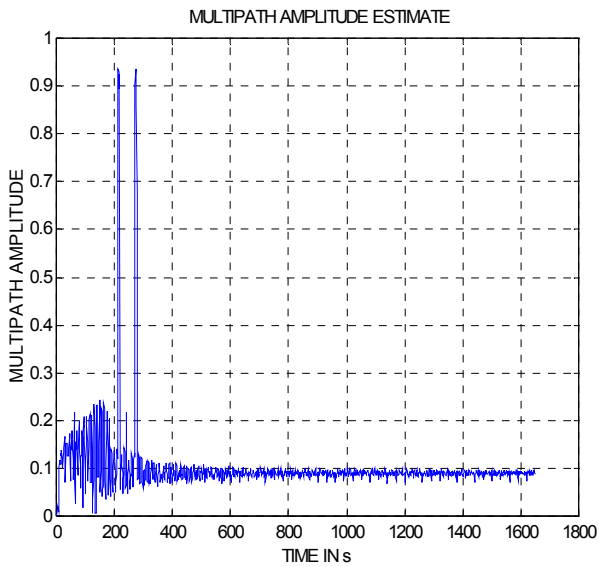


Figure 4.9 Multipath amplitude estimation performance with ‘trailing edge’ receiver configuration for  $\alpha = 0.1$  as a function of time in the run (multipath delay varies by 0.02 chip every 30 s).

As we can see in figure 4.8, the time delay estimation is not very robust until the multipath delay is larger than 0.2 chip. In addition, when the multipath delay is larger than 1 chip, the estimate is noisy. As shown in figure 4.9, the multipath amplitude estimate is not robust until the time delay is larger than 0.2 chip.

Figures 4.10 and 4.11 show the time delay and amplitude estimation performance using the ‘peak intensive’ receiver configuration. We see that with that receiver

configuration, the time delay and amplitude estimate are robust when the multipath delay is larger than 0.06 chip, which is a very good performance.

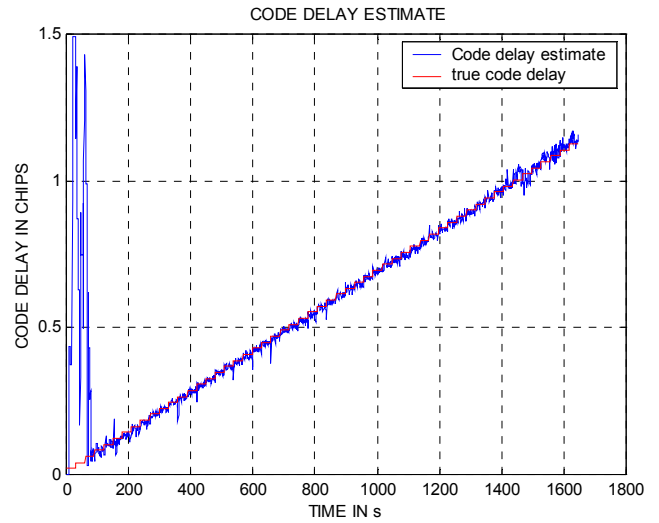


Figure 4.10 Multipath time delay estimation performance with ‘peak intensive’ distribution for  $\alpha = 0.1$  as a function of time in the run (multipath delay varies by 0.02 chip every 30 s).

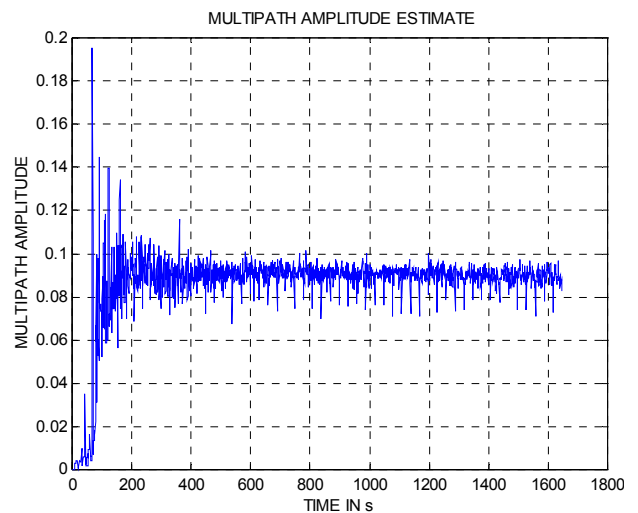


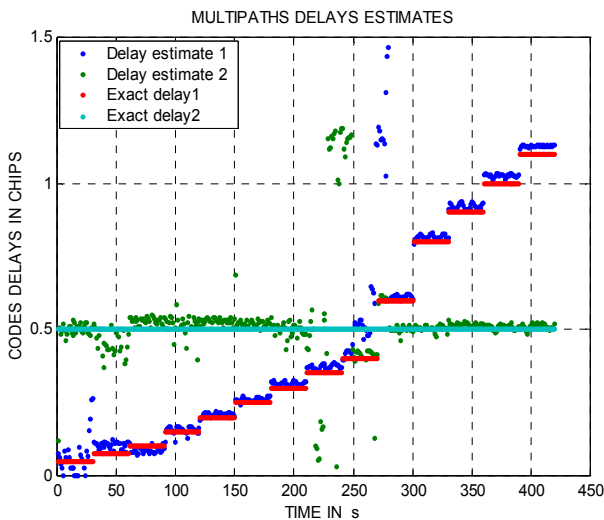
Figure 4.11 Multipath amplitude estimation performance with ‘peak intensive’ distribution for  $\alpha = 0.1$  as a function of time in the run (multipath delay varies by 0.02 chip every 30 s).

Therefore, the proposed technique provides a reliable estimate of the multipath time delay, amplitude and phase when the multipath time delay is larger than 0.06 chip using the ‘peak intensive’ receiver configuration. In addition, we have shown that the code and phase tracking errors have a consistent behaviour (quadrature) and do fit closely to their theoretical envelope.

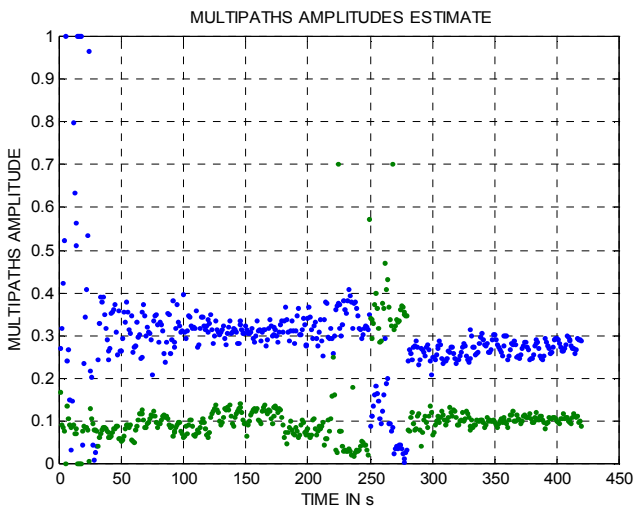


### 4.3 Scenario with two reflected rays

In this case, two reflected rays are considered: the first one has a fixed time delay equal to 0.5 chip when the time delay of the second ray varies every 30 s and is equal to 0.05, 0.075, 0.1, 0.15, 0.2, 0.25, 0.3, 0.35, 0.4, 0.6, 0.8, 0.9, 1.0, 1.1, 1.2 chip. The multipath amplitude of the first fixed ray is equal to 0.1, and the amplitude of the varying ray is set to 0.3. Time delay estimates and amplitude estimates are shown in figures 4.12 and 4.13 for the ‘uniform’ receiver configuration.



Figures 4.12 Multipath time delay estimation performance with ‘uniform’ distribution for  $\alpha_1=0.1$ ,  $\alpha_2=0.3$  as a function of time in the run (ray 1 delay is constant equal to 0.5 chip, ray 2 delay is as presented above).

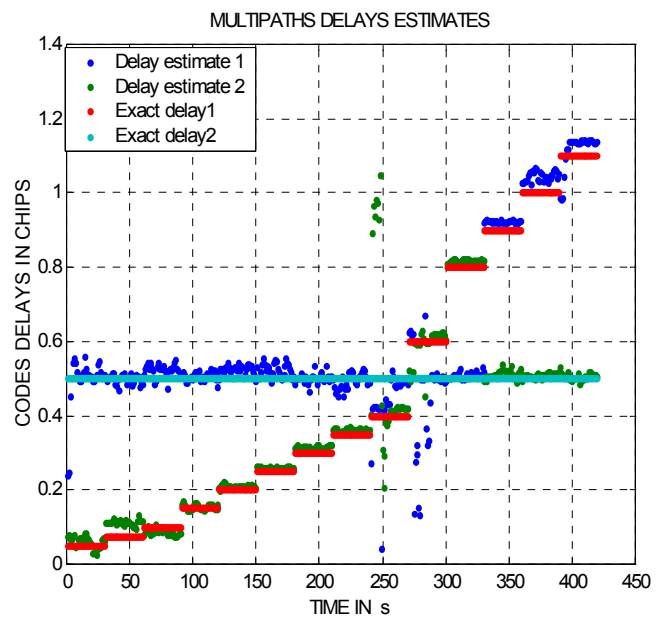


Figures 4.13 Multipath amplitude estimation performance with ‘uniform’ distribution for  $\alpha_1=0.1$ ,  $\alpha_2=0.3$  as a function of time in the run (ray 1 delay is constant equal to 0.5 chip, ray 2 delay is as presented above).

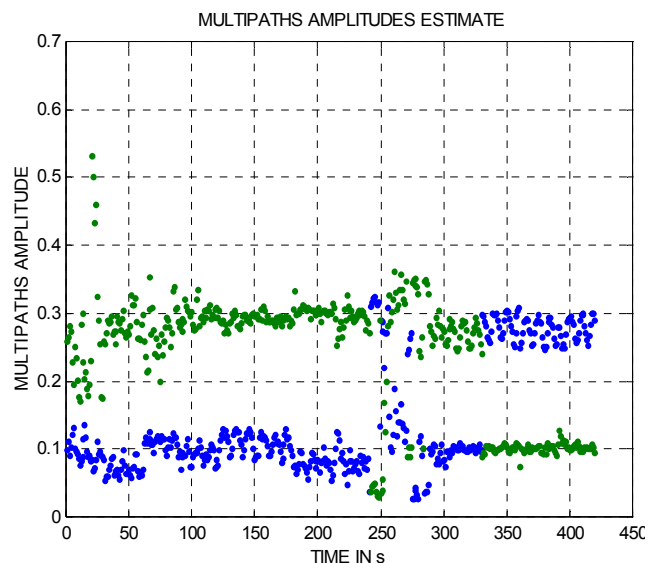
It is clear that even if the algorithm is able to estimate reflected rays parameters with the same accuracy as in the case of one

reflected ray, its performance collapse when the two reflected rays have slightly the same time delay due to the fact that the observation function is not injective. We can also see by the color change that the parameters estimates relative to each are often interchanged by the algorithm.

Figures 4.14 and 4.15 show time delay estimates and amplitude estimates for the ‘peak intensive’ receiver configuration. As we can see, the estimate is less affected by noise and is more robust for a short delay of ray 2 and when both delays are identical. Note again that the parameters estimates relative to each are often interchanged by the algorithm.



Figures 4.14 Multipath time delay estimation performance with ‘peak intensive’ distribution for  $\alpha_1=0.1$ ,  $\alpha_2=0.3$  as a function of time in the run (ray 1 delay is constant equal to 0.5 chip, ray 2 delay is as presented above).



Figures 4.15 Multipath amplitude estimation performance with ‘peak intensive’ distribution for  $\alpha_1=0.1$ ,  $\alpha_2=0.3$  as

*a function of time in the run (ray 1 delay is constant equal to 0.5 chip, ray 2 delay is as presented above).*

## **5. CONCLUSION**

This paper has presented a least squares technique for multipath parameters identification and code and phase tracking error estimation using a multicorrelator receiver.

In the case of one reflected ray, the technique is able to estimate the multipath parameters (time delay, relative amplitude, phase shift) with good accuracy (better than 0.05 chip for code delay, better than 0.05 for relative amplitude) when the multipath delay is strictly larger than 0.06 chip. The technique also provides estimates of the code and phase tracking errors that seem to have a consistent behaviour and fit perfectly in their theoretical envelope.

In the case of 2 reflected rays, the multipath parameters are estimated with the same accuracy, although the technique is not robust when both multipath delays are identical because the observation function is not injective.

Potential applications are twofold: siting and more generally channel characterization through identification of multipath parameters, tracking performance improvement through removal of multipath components from tracking loops discrimination functions. Note that the current limitation here is on the relative delay of all rays (strictly larger than 0.06 chip) and on the multipath relative amplitude (larger than 0.05).

Further work aim at testing this technique on live signals and at refining the estimation technique to reduce those limits.

## **ACKNOWLEDGMENTS**

The authors wish to thank Diane Rambach for her help during the evaluation of the performance of the proposed algorithm on live measurements.

## **REFERENCES**

[1] Van Nee R., Sierveld J., Fenton P. and Townsend B. (1994) «The Multipath Estimating Delay Lock Loop: Approaching Theoretical Limits», proceedings of IEEE PLANS 94, Las Vegas, April 11-15.

[2] Braasch M. (1996) «Global Positioning System: Theory and Applications», volume 1, chapter 'Multipath Effects', pages 547-568, AIAA.

[3] Fenton P., Falkenberg B., Ford T., Ng K. and Van Dierendonck A.J. (1991) «NovAtel's GPS Receiver – the High Performance OEM Sensor of the Future», proceedings of ION GPS-91, Albuquerque, Sept 9-13.

[4] Van Dierendonck A.J., Fenton P. and Ford T. (1992) «Theory and Performance of Narrow Correlator Spacing in a GPS Receiver», proceedings of ION National Technical Meeting, San Diego, January 27-29.